RSC Advances

PAPER

View Article Online
View Journal | View Issue

Cite this: *RSC Adv.*, 2017, **7**, 12474

A promising vanadium sulfide counter electrode for efficient dye-sensitized solar cells

Xianqing Liu, Gentian Yue* and Haiwu Zheng*

Received 25th December 2016
Accepted 6th February 2017

DOI: 10.1039/c6ra28667d

rsc.li/rsc-advances

In this study, we demonstrated the synthesis of vanadium sulfide (VS_2) *via* an *in situ* hydrothermal route, which was subsequently employed as a counter electrode (CE) for Pt-free dye-sensitized solar cells (DSSCs) for the first time. It was demonstrated from scanning electron microscopy that the size of VS_2 increased with the increasing temperature, and the morphology was also affected by temperature. Extensive electrochemical performance analysis, including cyclic voltammetry, electrochemical impedance, and Tafel polarization, revealed that the VS_2 CE possesses a high electrocatalytic activity for the reduction of triiodide to iodide and a low charge-transfer resistance at the electrolyte/CE interface. The DSSC based on the VS_2 CE exhibited a conversion efficiency of 6.24% under an illumination of 100 mW cm^{-2} as compared to the DSSC based on the Pt CE.

1. Introduction

Dye-sensitized solar cells (DSSCs) have received extensive interest due to their facile fabrication, sustainability, low-cost, and environmentally friendliness.[1–4] The typical structure of a DSSC consists of TiO_2 nanocrystallines as the photoanode, dyes, and a platinum (Pt)-coated tin oxide transparent (FTO) substrate as the counter electrode (CE) fabricated with an I^-/I_3^- redox couple liquid electrolyte.[5] Although Pt is one of the most selected materials for catalyzing the reduction of I_3^- to I^- due to its superior electrocatalytic ability, stability, and conductivity, as a noble metal, its high cost restricts the scale up production for DSSCs. To resolve this issue, many researchers are concentrating on CE catalytic materials, including carbon-based materials, metal sulfides, nitrides, polymers, and oxides,[8–10] with a high conductivity, large specific surface areas, and a good catalytic ability.[6,7] Among these, metal sulfides with two-dimensional (2D) permeable channels possess the properties of ideal CE materials and are considered as promising electrode materials.[11,12] Lin *et al.*[13] prepared a molybdenum disulfide CE for DSSCs and obtained a significant improvement in the power conversion efficiency. Moreover, we also successfully prepared a nickel disulfide CE with very promising results for DSSCs.[13,14] Vanadium sulfide (VS_2) has been proven to be an ideal material platform due to its synergic properties of metallic nature brought about by the conducting S–V–S layers stacked up *via* weak van der Waals interlayer interactions, offering great potential as high-performance in-plane supercapacitor electrodes.[15] Therefore, it is interesting and significant to investigate the potential applications of VS_2 as a CE catalyst in DSSCs for low-cost and efficient photoelectric conversion efficiency.

Herein, we designed and synthesized VS_2 nanofibres as a CE material *via* an *in situ* hydrothermal route for DSSCs, hoping that the VS_2 nanofibres could promote the catalytic activity and improve the photovoltaic properties of the DSSC. The DSSC based on the VS_2 nanofibre CE exhibited a high power conversion efficiency of 7.40%. This study may broaden the potential applications of two-dimensional layered transition-metal dichalcogenides in the area of photoelectrochemistry.

2. Experimental

2.1 Preparation of VS_2 CEs

VS_2 was prepared *via* modifying the procedure reported by Feng *et al.*[15] A 3 mmol sodium orthovanadate and 15 mmol thiourea were dissolved in 40 ml distilled water; the mixture was then stirred for 1 h to form a homogeneous solution and transferred to a 50 ml Teflon-lined autoclave. It was then heated in an oven at 140, 160, 180, and 200 °C for 24 h. The product was collected by centrifugation, washed at least 5 times with ethanol and distilled water, and dried in a vacuum oven at 80 °C for 12 h. The slurry of the VS_2 CE was composed of nanofibre structure VS_2, acetylene black, and polyvinylidene fluoride (weigh ratio = 8 : 1 : 1), which were dissolved in *N*-methyl-2-pyrrolidinone. Then, the slurry was ultrasonicated for 30 min and was stirred for 12 h. Subsequently, the as-prepared slurry was coated on the FTO substrates using a doctor blade method. The coated CEs were dried at 100 °C for 24 h in a vacuum oven.

2.2 Fabrication of the DSSCs

A TiO_2 anode was prepared according to a previously reported procedure.[16,17] The dye-sensitized TiO_2 photoanode was

Henan Key Laboratory of Photovoltaic Materials and Laboratory of Low-Dimensional Materials Science, Henan University, Kaifeng 475004, China. E-mail: yuegentian@henu.edu.cn; zhenghaiw@ustc.edu; Tel: +86 371 23880696

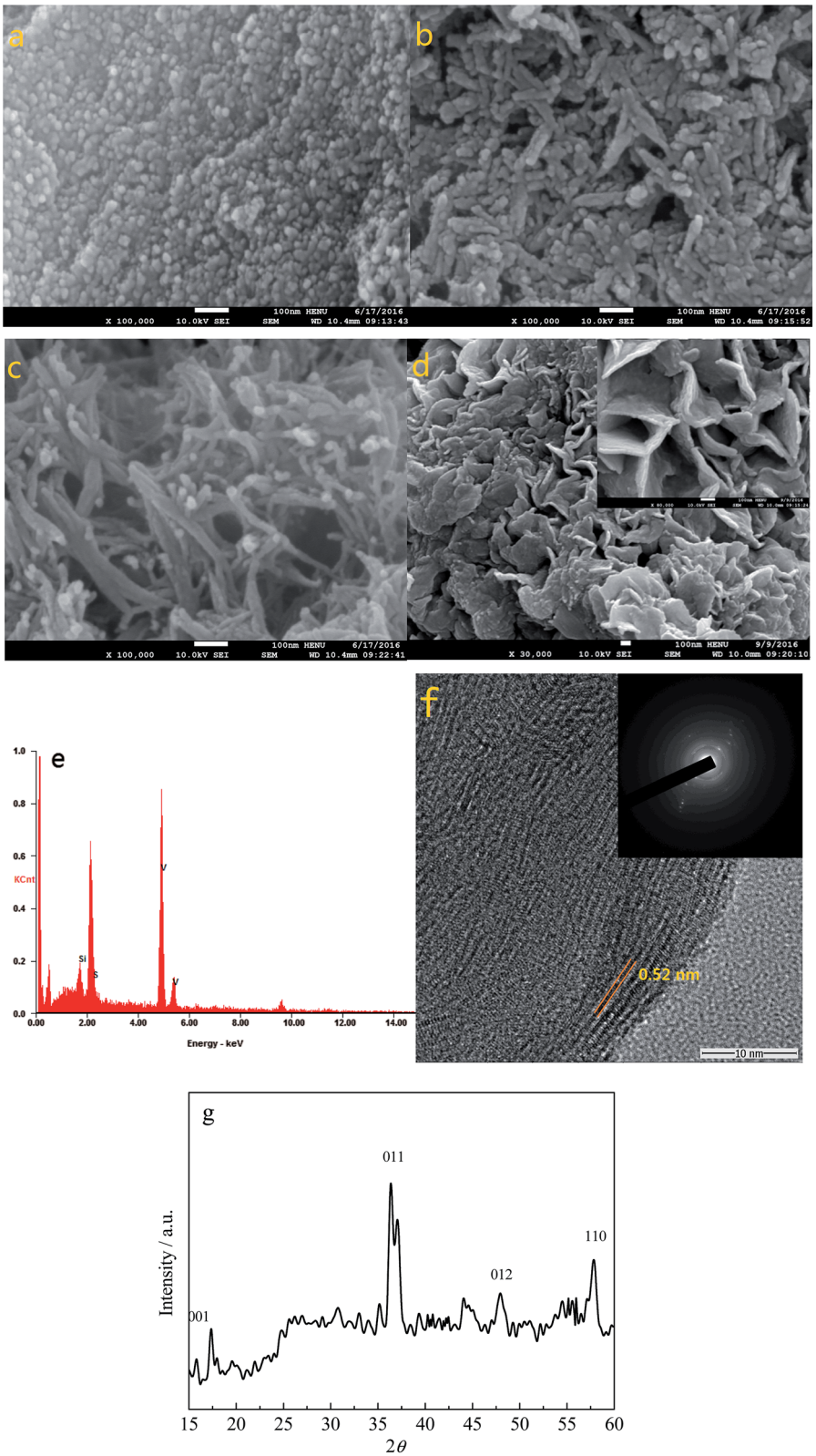

Fig. 1 The SEM images of VS_2 obtained at (a) 140 (b) 160, (c) 180, and (d) 200 °C; (e) the EDS spectrum of VS_2; (f) TEM image of the VS_2 obtained after the 180 °C hydrothermal synthesis; (g) XRD pattern of the VS_2 nanofibers.

constructed by immersing the TiO_2 photoanode in a 0.3 mM dye Z907 ethanol solution for 24 h. Thus, a dye-sensitized TiO_2 photoanode with a total thickness of 6–8 μm was obtained. After this, the dye-sensitized TiO_2 photoanode and the CE were clipped together and wrapped with the thermoplastic hot-melt Surlyn. The liquid electrolyte contained 0.05 M of iodine,

0.1 M of lithium iodide, 0.6 M of tetrabutylammonium iodide, and 0.5 M of 4-*tert*-butyl-pyridine in acetonitrile and was injected into the aperture between the two electrodes.

2.3 Characterization

The surface morphology of the sample was observed using a JSM-7001F field emission scanning electron microscope (SEM). Energy dispersive spectroscopy analysis (EDS) was carried out using a Bruker-ASX (Model Quan-Tax 200). A field emission transmission electron microscope (TEM; JEOL JEM-2100F, operated at 200 kV with a point-to-point resolution of 0.19 nm) was used to obtain information about the microstructures. The crystalline structures of the composites were investigated by glancing incidence X-ray diffractometer (X'Pert Pro, PANalytical B.V., the Netherlands). Electrochemical impendence spectroscopy (EIS) was carried out using a CHI660E (Shanghai Chenhua Device Company, China) electrochemical measurement system at a constant temperature of 25 °C in an ambient atmosphere under dark conditions, leaving an exposed area of 0.8 cm^2. The frequency of the applied sinusoidal AC voltage signal was varied from 0.1 Hz to 10^5 Hz, and the corresponding amplitude was set at 5 mV in all the cases.

The photovoltaic test of the DSSC with an exposed area of 0.2 cm^2 was carried out by measuring photocurrent–photovoltage (*J*–*V*) character curves under a white light irradiation of 100 mW cm^{-2} (AM 1.5 G) from a solar simulator (CEL-S500, Beijing China Education Au-light Co., Ltd) in an ambient atmosphere.

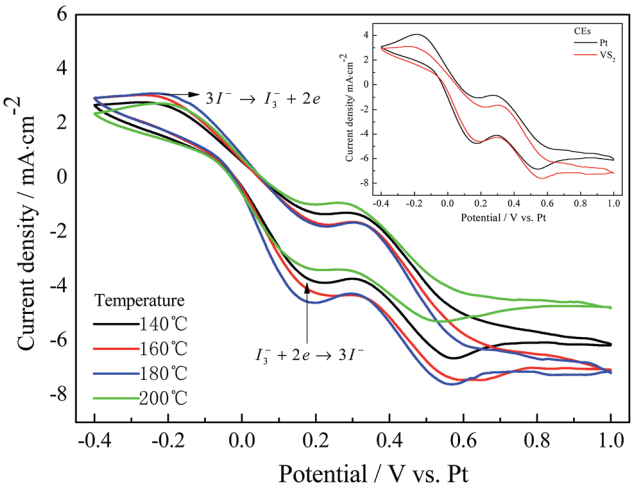

Fig. 2 Cyclic voltammograms for the Pt and VS_2 (prepared at 140 °C to 200 °C) CEs.

3. Results and discussion

Fig. 1a–d show the SEM images of VS_2 obtained at 140, 160, 180, and 200 °C, respectively. It can be seen that the size of the VS_2 nanoparticles increased with the increasing temperature and the morphology also changed, from nanoparticles to nanofibers and nanosheets. This phenomenon indicates that a higher reaction temperature can promote the growth of VS_2 crystals. The EDS patterns of VS_2 prepared at 180 °C are shown in Fig. 1e, in which the V and S elements with an almost 1 : 1 ratio can be detected, and the Si element originates from the Si substrate. Fig. 1f presents the TEM image of VS_2, and the lattice spacing has been estimated to be 0.52 nm, which is in accordance with the literature parameter for VS_2 (0.573 nm). To further identify the composition of the sample, Fig. 1g shows the XRD pattern of the VS_2 nanofibers obtained from the 180 °C hydrothermal synthesis. As can be seen, although there are some impurity peaks appearing in the sample, the (001), (011), (012), and (110) peaks of the VS_2 all correspond to the JCPDS database card no. 89-1640. As a consequence, the results demonstrated that the VS_2 has been successfully prepared *via* the facile hydrothermal synthesis at 180 °C.

Fig. 2 presents the cyclic voltammograms of various CEs measured using a three-electrode system. In Fig. 2, the pair of peaks in the low potential area has a significant impact on the photovoltaic properties of the DSSCs between the two pairs of redox peaks.[18] As observed from the inset of Fig. 2, the Pt and VS_2 (180 °C preparation) CEs have a similar cathodic peak current density (J_{pc}) and cathodic peak potential, indicating that the VS_2 CE is as good conductive and catalytic material as Pt. The VS_2 CEs prepared at temperatures from 140 to 200 °C possess a similar cathodic peak potential, and the cathodic peak current density follows the order VS_2 (180 °C) > VS_2 (160

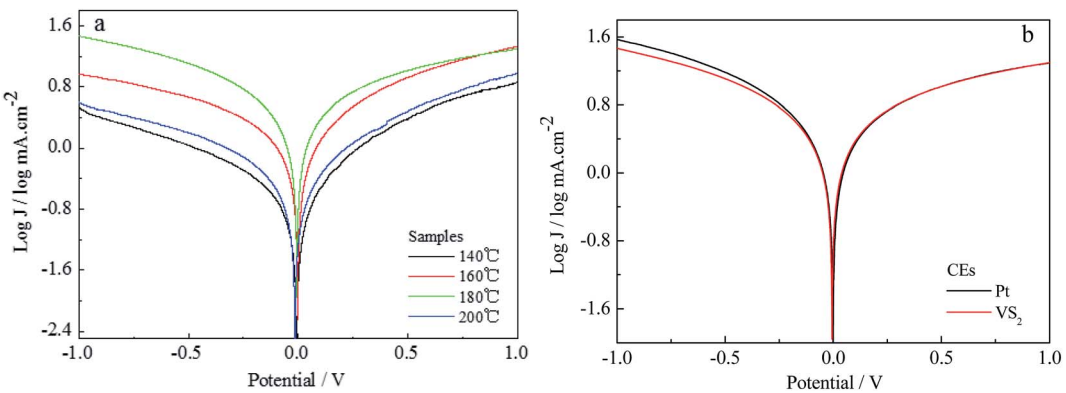

Fig. 3 Tafel curves for (a) various VS_2 CEs and (b) the Pt CE and the VS_2 CE prepared at 180 °C.

°C) > VS_2 (140 °C) > VS_2 (200 °C) CEs, suggesting that the VS_2 CE prepared at 180 °C has a better catalytic activity and conductivity. This indicates that the electron transport was affected by the surface morphologies of the samples. VS_2 nanofibers with a large specific surface area can vastly enhance the accessibility of the electrolyte to the electrode, thus improving interfacial charge transfer and increasing the number of active catalytic sites.[19,20]

Tafel curves for the VS_2 CEs prepared at different temperature are shown in Fig. 3a. The exchange current density (J_0), obtained as the intercept of the extrapolated linear region of the curve when the overpotential was zero, is positively correlated to the reduction capability of the CE materials in an I^-/I_3^- electrolyte. The VS_2 CEs prepared at temperatures from 140 to 200 °C exhibit the same change tendencies as for the CVs. Under the optimizing conditions, the J_0 of the VS_2 CE (180 °C preparation) is similar to that of the Pt CE, as shown in Fig. 3b. This is mainly because VS_2 (180 °C preparation) with nanofibre structure is better for electron transport than VS_2 nanoparticles. Thus, this also indicates that the electrochemical catalytic activity of the VS_2 CE is significantly affected by the morphology.

Fig. 4 displays the electrochemical impedance spectroscopy (EIS) and equivalent circuit models of the Pt and the VS_2 CEs synthesized at various temperatures, in which the first semicircle in the high frequency region denotes the charge-transfer resistance (R_{ct}) at the CE/electrolyte interface[21,22] and the corresponding EIS parameters are listed in Table 1. The smaller R_{ct} exhibits a faster electron transfer from the CE to the electrolyte, which is a significant parameter for evaluating the performance of CEs. In Fig. 4, the values of R_{ct} for the VS_2 CEs synthesized at 140, 160, 180 and 200 °C are 6.437, 4.318, 3.360, and 8.435 Ω cm^2, respectively; and the R_{ct} for the Pt CE is 3.432 Ω cm^2. The R_{ct} value for the VS_2 CE prepared at 180 °C is comparable to that of the Pt CE. The results are in agreement with the CVs and Tafel curves, and this can be attributed to the same reasons as for the CVs and Tafel curves.

Fig. 5 shows the photocurrent density–voltage curves for the DSSCs based on the Pt and VS_2 (180 °C preparation) CEs under the irradiation of 100 mW cm^{-2}, and the photovoltaic parameters for the DSSCs are also summarized in Table 1. From Fig. 5, it can be observed that the DSSC based on the VS_2 CE synthesized at 180 °C achieved a power conversion efficiency (PCE) of 6.24%, an open-circuit voltage (V_{oc}) of 0.726 V, a short-circuit current density (J_{sc}) of 13.65 mA cm^{-2}, and a fill factor (FF) of 0.63, which are almost the same as those for the DSSC based on the Pt electrode (PCE = 6.44%, V_{oc} = 0.717 V, J_{sc} = 14.03 mA cm^{-2}, and FF = 0.64). The DSSCs based on the VS_2 CEs prepared at 140, 160 and 200 °C have much lower PCEs than the DSSC with the VS_2 CE synthesized at 180 °C. The positive effect in the performance of the DSSC based on the VS_2 (180 °C) CE possibly results from the following aspects. First, the contact frequency between the I^-/I_3^- redox couple in the electrolyte and the CE can be quickened because of the large specific surface area of

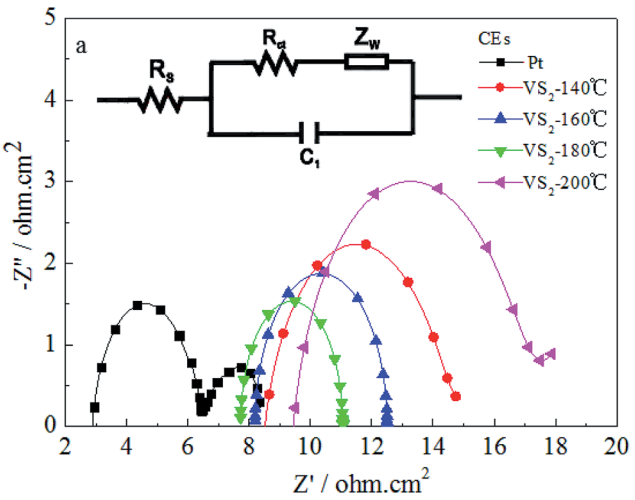

Fig. 4 EIS spectra for the Pt and VS_2 CEs. The inset (a) shows the equivalent circuit model used for fitting the resultant impedance spectra.

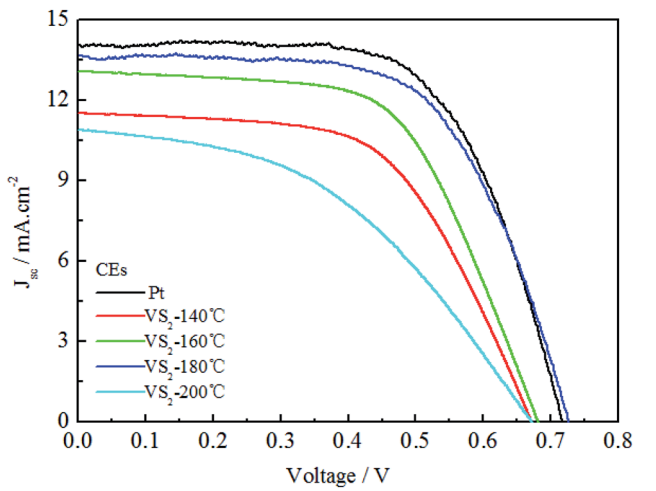

Fig. 5 Photocurrent density–voltage curves of the DSSCs based on Pt and various VS_2 CEs.

Table 1 Electrochemical parameters for the Pt and VS_2 CEs and the corresponding photocurrent–voltage parameters of the DSSCs

Temp. (°C)	R_{ct} (Ω cm^2)	$\|J_{pc}\|$ (mA cm^{-2})	V_{oc} (V)	J_{sc} (mA cm^{-2})	FF	η (%)
140	6.437	3.79	0.671	11.52	0.58	4.48
160	4.318	4.20	0.681	13.06	0.60	5.34
180	3.360	4.55	0.726	13.65	0.63	6.24
200	8.435	3.33	0.672	10.89	0.46	3.37
Pt	3.432	4.65	0.717	14.03	0.64	6.44

the VS_2 nanofibers, such that to provide a good reaction speed for the reduction of I_3^- to I^-. In addition, the VS_2 nanofibers have synergic advantages of a high conductivity and 2D permeable channels guarantee the rapid transmission of electrons, thereby showing efficient PCEs for the DSSCs based on the VS_2 CE. In addition, it has been reported in previous studies that VS_2 was successfully assembled for constructing the electrodes of in-plane supercapacitors.[23,24] To the best of our knowledge, it is the first time that VS_2 has been reported as a CE material for DSSCs.

4. Conclusion

VS_2 nanofibers were prepared *via in situ* hydrothermal techniques and were employed as a CE in the Pt-free DSSCs for the first time. The sizes of VS_2 increase and the morphology is also affected with the increasing temperature, whereby nanoparticles were observed to changed into nanofibers and even nanosheets. Extensive electrochemical and photoelectric chemical experiments indicate that the VS_2 nanofibers prepared at 180 °C have the synergic advantages of high conductivity, large specific surface area, and 2D permeable channels and provide the most excellent catalytic activity for the reduction of triiodide compared to VS_2 prepared at 140, 160, and 200 °C. Under the optimum conditions, the PCE of the DSSC based on the VS_2 nanofiber CE (6.24%) is as high as that of the DSSC based on the Pt electrode (6.44%). This study offers a new and effective material substitution to Pt, which will broaden the application field of 2D sulfides.

Conflict of interest

The authors declare that they have no competing interests.

Acknowledgements

The authors are very grateful for the joint support by the National Natural Science Foundation of China (No. U1504624). This work was also supported by the China Postdoctoral Science Foundation Funded Project (No. 2015M572102).

References

1 B. O'Regan and M. Grätzel, *Nature*, 1991, **353**, 737–740.
2 A. Yella, H. W. Lee, H. N. Tsao, C. Y. Yi, A. K. Chandiran, M. K. Nazeeruddin, E. W. G. Diau, C. Y. Yeh, S. M. Zakeeruddin and M. Grätzel, *Science*, 2011, **334**, 629–634.
3 A. Hagfeldt, G. Boschloo, L. Sun, L. Kloo and H. Pettersson, *Chem. Rev.*, 2010, **110**, 6595–6663.
4 S. Mathew, A. Yella, P. Gao, R. Humphry-Baker, B. F. E. Curchod, N. Ashari-Astani, I. Tavernelli, U. Rothlisberger, M. K. Nazeeruddin and M. Grätzel, *Nat. Chem.*, 2014, **6**, 242–247.
5 J. H. Wu, Z. Lan, J. M. Lin, M. L. Huang, Y. F. Huang, L. Q. Fan and G. G. Luo, *Chem. Rev.*, 2015, **115**, 2136–2173.
6 Y. J. Li, Q. W. Tang, L. M. Yu, X. F. Yan and L. Dong, *J. Power Sources*, 2016, **305**, 217–224.
7 G. T. Yue, X. P. Ma, W. F. Zhang, F. M. Li, J. H. Wu and G. Q. Li, *Nanoscale Res. Lett.*, 2015, **10**, 1–9.
8 Z. Q. Li, F. Gong, G. Zhou and Z. S. Wang, *J. Phys. Chem. C*, 2013, **117**, 6561–6566.
9 H. C. Sun, D. Qin, S. Q. Huang, X. Z. Guo, D. M. Li, Y. H. Luo and Q. B. Meng, *Energy Environ. Sci.*, 2011, **4**, 2630–2637.
10 G. T. Yue, P. Li, F. M. Li and C. Chen, *RSC Adv.*, 2016, **6**, 61278–61283.
11 M. Mulazzi, A. Chainani, N. Katayama, R. Eguchi, M. Matsunami, H. Ohashi, Y. Senba, M. Nohara, M. Uchida, H. Takagi and S. Shin, *Phys. Rev. B: Condens. Matter Mater. Phys.*, 2010, **82**, 075130.
12 K. S. Kim, Y. Zhao, H. Jang, S. Y. Lee, J. M. Kim, K. S. Kim, J. H. Ahn, P. Kim, J. Y. Choi and B. H. Hong, *Nature*, 2009, **457**, 706–710.
13 J. Y. Lin, A. L. Su, C. Y. Chang, K. C. Hung and T. W. Lin, *ChemElectroChem*, 2015, **2**, 720–725.
14 G. T. Yue, F. R. Tan, F. M. Li, C. Chen, W. F. Zhang, J. H. Wu and Q. H. Li, *Electrochim. Acta*, 2014, **149**, 117–125.
15 J. Feng, X. Sun, C. Z. Wu, L. L. Peng, C. W. Lin, S. L. Hu, J. L. Yang and Y. Xie, *J. Am. Chem. Soc.*, 2011, **133**, 17832–17838.
16 G. T. Yue, J. H. Wu, Y. M. Xiao, M. L. Huang, J. M. Lin and J.-Y. Lin, *J. Mater. Chem. A*, 2013, **1**, 1495–1501.
17 Z.-Q. Li, Y.-P. Que, L.-E. Mo, W.-C. Chen, Y. Ding, Y.-M. Ma, L. Jiang, L.-H. Hu and S.-Y. Dai, *ACS Appl. Mater. Interfaces*, 2015, **7**, 10928–10934.
18 G. T. Yue, J. H. Wu, J.-Y. Lin, Y. M. Xiao, J. M. Lin, M. L. Huang and Z. Lan, *Carbon*, 2013, **55**, 1–9.
19 C.-T. Li, Y.-L. Tsai and K.-C. Ho, *ACS Appl. Mater. Interfaces*, 2016, **8**, 7037–7046.
20 H. Sun, J. Deng, L. Qiu, X. Fang and H. Peng, *Energy Environ. Sci.*, 2015, **8**, 1139–1159.
21 Y. Xiao, G. Han, Y. Li, M. Li and Y. Chang, *J. Mater. Chem. A*, 2014, **2**, 3452–3460.
22 G. Yue, J. Wu, Y. Xiao, J. Lin, M. Huang and Z. Lan, *J. Phys. Chem. C*, 2012, **116**, 18057–18063.
23 D. Pech, M. Brunet, H. Durou, P. Huang, V. Mochalin, Y. Gogotsi, P. L. Taberna and P. Simon, *Nat. Nanotechnol.*, 2010, **5**, 651–654.
24 J. J. Yoo, K. Balakrishnan, J. Huang, V. Meunier, B. G. Sumpter, A. Srivastava, M. Conway, A. L. Mohana Reddy, J. Yu, R. Vajtai and P. M. Ajayan, *Nano Lett.*, 2011, **11**, 1423–1427.

